

# Surface and sub-surface investigations of the plasma influence on Cs doped Mo as surface converter for negative hydrogen ion sources for fusion

L. SCHIESKO<sup>(a)1</sup>, S. CRISTOFARO<sup>2</sup>, T. HÖSCHEN<sup>2</sup> and C. HOPF<sup>2</sup>

<sup>1</sup> *Laboratoire de Physique des Gaz et Plasmas—LPGP, UMR 8578 CNRS, Université Paris-Sud, Université Paris-Saclay, F-91405 Orsay Cedex, France*

<sup>2</sup> *Max-Planck-Institut für Plasmaphysik, Boltzmannstrasse 2, D-85748 Garching, Germany*

PACS 52.00.00 –  
PACS 82.80.Pv –

**Abstract** – The influence of low pressure and low temperature hydrogen plasma on a pure molybdenum sample implanted with caesium is investigated by means of sputtering-XPS. A portion of the sample was exposed to the plasma, while the rest of the sample was covered by stainless steel and thus shielded from direct plasma flux. The results show that the part of the sample exposed to the plasma exhibits both on and beneath the surface an increased amount of H<sub>2</sub>O and MoO<sub>2</sub> with respect to the covered sample part which can be explained by a chemical reduction of MoO<sub>3</sub> oxides by the hydrogen plasma species. The XPS Cs lines show oxidation peaks. A sputtering depth of roughly 13 nm is necessary to recover identical spectrum, indicating that the plasma changes the chemical composition of the implanted samples not only on the surface but also inside the material.

Negative hydrogen ion sources for ITER neutral beam injectors [1–4] are based on the conversion of neutral and positive hydrogen ion species (H<sup>0</sup>/D<sup>0</sup> and H<sub>x</sub><sup>+</sup>/D<sub>x</sub><sup>+</sup>, x=1...3) into negative ions H<sup>−</sup>/D<sup>−</sup> on a converter surface. The negative ion generation yield is greatly enhanced by in-situ evaporation of Cs [5,6] as it reduces the work function of the surfaces on which it is deposited.

At the negative ion test beds of IPP Garching [1,2], the Cs is evaporated from an oven, containing 1 g ampullae of liquid Cs. The evaporation of Cs leads to an increase of the source performance, i.e., an increase of the extracted H<sup>−</sup>/D<sup>−</sup> current density and a reduction of the inevitably co-extracted electrons (see for example [7]). However, the Cs layers are slowly passivated over time by impurities such as oxygen and nitrogen due to the base vacuum being around 5x10<sup>−7</sup> mbar and, additionally the plasma slowly erodes the Cs layers deposited on the surface.

These two effects lead to a decrease of the source performance which can be counterbalanced by continually

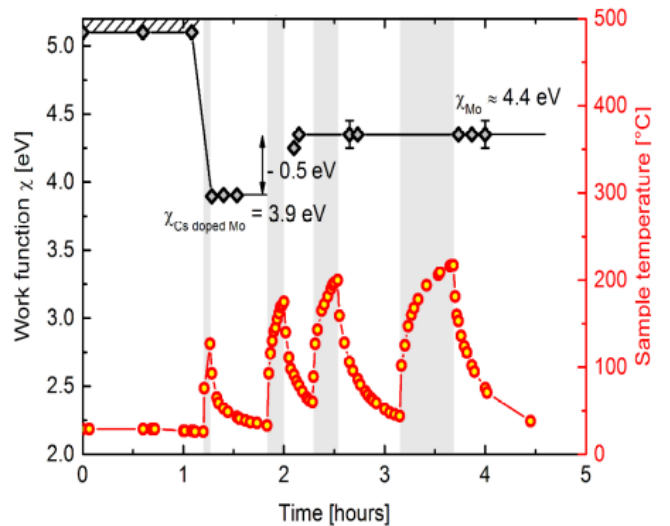


Fig. 1: Variation of the plasma exposed sample part WF and temperature as a function of time. The grey-shadowed parts represent hydrogen plasma pulses at a pressure of 10 Pa H<sub>2</sub>, and an injected RF power of 250 W.

<sup>(a)</sup>Work carried out at Max-Planck-Institut für Plasmaphysik

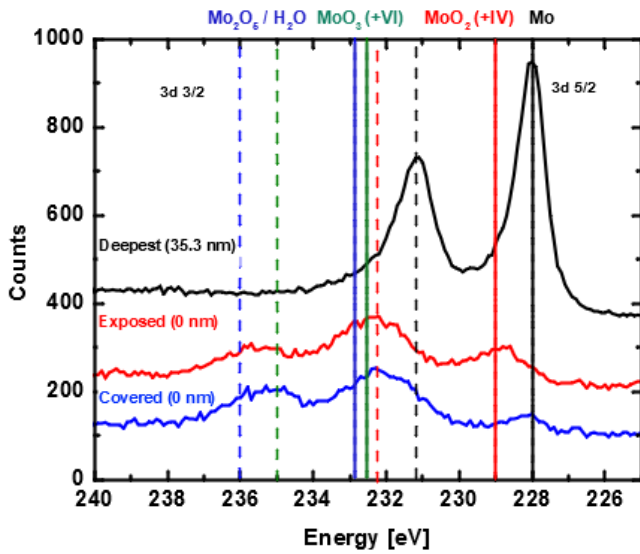


Fig. 2: High-resolution XPS spectra of the Mo valence bands for the covered and plasma exposed sample parts measured at the surface (0 nm) and after a of fluence  $3.59 \times 10^{16} \text{ Ar}^+$  ions (evaluated depth of 35.3 nm)

for the exposed sample part. The location of the 3d 3/2 and 3d 5/2 valence bands is indicated in dashed and full lines respectively for  $\text{Mo}_2\text{O}_5 / \text{H}_2\text{O}$ ,  $\text{MoO}_3$  (+VI),  $\text{MoO}_2$  (+IV) and Mo. The oxidation state of the Mo oxides is indicated in parenthesis. A count offset has been used to improve the readability.

evaporating fresh Cs from the ovens. The Cs consumption, for sources equipped with one driver [1], was determined to range between 2 and 5 mg/h [8,9]. As already shown [10,11], a proposed strategy to reduce the Cs consumption is to implant Cs into the plasma facing component of the converter surface of the negative hydrogen ion source, made of molybdenum.

In this letter, the results obtained by implanting Cs into Mo are reviewed and then the properties of this material and the changes induced by hydrogen plasma are investigated.

Preliminary studies with a small amount of implanted Cs ( $5 \times 10^{15} \text{ cm}^{-2}$  Cs atoms at 15 keV energy followed by  $5 \times 10^{15} \text{ cm}^{-2}$  Cs atoms at 10 keV energy) leading to 5% surface Cs atomic concentration, were conducted [10, 11]. The surface generation mechanisms, namely the sputtering of an adsorbed hydrogen atom as  $\text{H}^-$  and the backscattering as  $\text{H}^-$  of plasma positive ions on the implanted surface, have been clearly identified. Furthermore, it has been experimentally shown that under a low positive ion flux (around  $10^{18} \text{ m}^{-2} \cdot \text{s}^{-1}$ ) the negative ion yield was stable over days and in particular during 4 h cw operation, provided that the sample exhibits a surface roughness, evaluated by profilometry, of around  $10 \text{ } \mu\text{m}$  peak to valley. One of the goals of the

first study was trying to reduce the work function (WF) of the implanted samples to a value around 2.8 eV. A comparison between the negative ion yield from pure Mo and Cs doped Mo samples allowed for an indirect estimate of the WF of the implanted sample ranging between 3.8 eV and 4.2 eV [10, 11] (pure Mo and Cs WF are 4.4 eV and 2.1 eV respectively). A comparison of X-ray photoelectron spectroscopy (XPS) depth profiling results conducted before and after plasma exposure showed hints of Cs diffusion, due to an increase of the sample temperature up to  $600^\circ\text{C}$  for less than 1 h.

In order to increase the surface Cs atomic concentration and study the surface and sub-surface mechanisms in hydrogen plasma with fluxes closer to the ones measured in negative hydrogen ion sources for fusion, it has been planned to implant new samples with an increased fluence and a reduced implantation energy when compared to the previous campaign [10, 11]. To achieve this goal, pure Mo samples were first prepared by sand blasting, and profilometry measurements showed a roughness of around  $10 - 17 \text{ } \mu\text{m}$  peak to valley. The samples were then implanted by an external company using the following two-step process:  $1.5 \times 10^{16} \text{ cm}^{-2}$  Cs atoms at 10 keV energy followed by  $10^{16} \text{ cm}^{-2}$  Cs atoms at 3 keV energy. The increase of the Cs fluence together with a reduction of the implantation energy, and thus of the sputtering yield, is expected to lead to an increase of the surface Cs atomic fraction and a shallower implantation profile. After implantation, the samples were left at atmospheric pressure and room temperature during a month before XPS analysis was possible. Stability of the implanted Cs left at atmospheric pressure and room temperature over a year has been observed [10, 11]. The samples were not prepared before implantation to remain as close as possible to the conditions that will occur in a negative ion source. As a consequence of not preparing the samples, the presence of both  $\text{MoO}_2$  and  $\text{MoO}_3$  oxides makes an accurate fit of the XPS spectra bands very difficult. The presence of  $\text{MoO}_3$  oxides is expected and very likely generated during the manufacturing process of the Mo plate that has been used for these experiments. For this reason, only the peak position is displayed in the panels 2 to 4. The evaluation of the Cs depth profile performed at the XPS experiment (described in Ref. [11]) on the samples as received after implantation showed profiles comparable to the ones obtained previously [10, 11] with a lower fluence and larger implantation energy, as well as roughly 5% Cs surface atomic concentration. The fact that no increase of the Cs surface atomic fraction was observed is likely due to a failure of the 3 keV step, as the implantation company reported difficulties at measuring very low implantation currents. The sample was partially covered by stainless steel and the work function of the plasma exposed Mo surface was measured at the ACCeS experiment (see [12] for detail) by photoelectron emission [13] as shown in Figure 1. Before plasma exposure

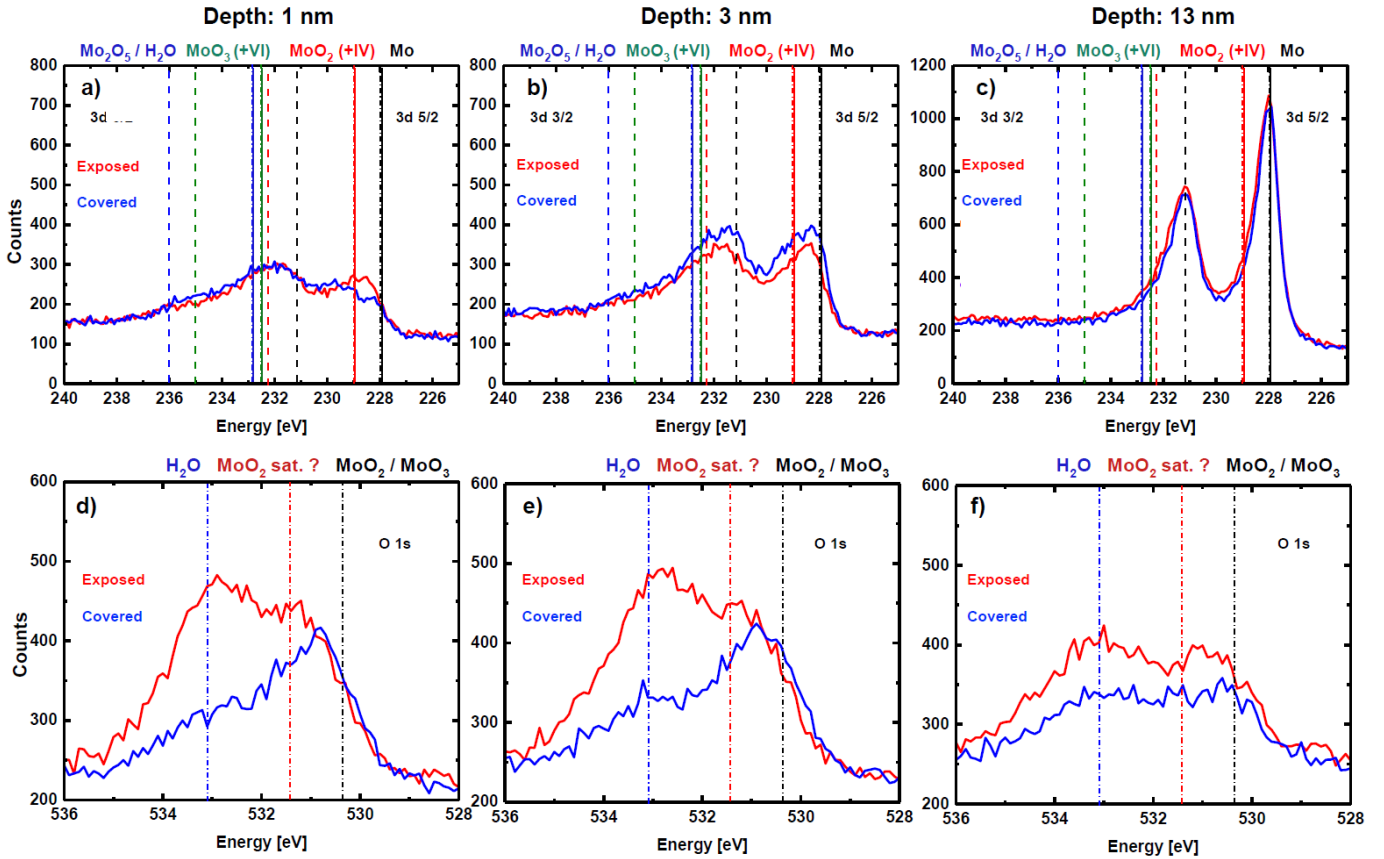


Fig. 3: High-resolution XPS spectrum of the Mo valence bands for the covered and plasma exposed sample parts measured at a fluence of a)  $1.04 \times 10^{15} \text{Ar}^+$  ions (evaluated depth of 1 nm), b)  $3.12 \times 10^{15} \text{Ar}^+$  ions (evaluated depth of 3 nm) and c)  $1.30 \times 10^{16} \text{Ar}^+$  ions (evaluated depth of 13 nm). The location of the 3d 3/2 and 3d 5/2 valence bands is indicated in dashed and full lines respectively for  $\text{Mo}_2\text{O}_5 / \text{H}_2\text{O}$ ,  $\text{MoO}_3 (+\text{VI})$ ,  $\text{MoO}_2 (+\text{IV})$  and Mo. The oxidation state of the Mo oxides is indicated in parenthesis. d), e) and f) present high-resolution XPS spectrum of the O 1s lines measured at a depth of 1 nm, 3 nm and 13 nm respectively. The location of  $\text{H}_2\text{O}$  band, a possible satellite band of  $\text{MoO}_2$  and the  $\text{MoO}_2 / \text{MoO}_3$  bands are indicated. For all the graphs, no count offset has been used.

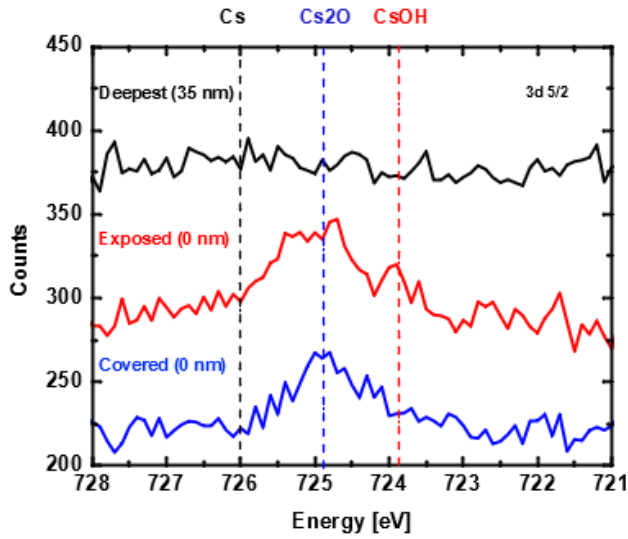


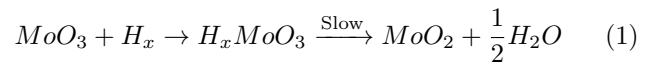
Fig. 4: High-resolution XPS spectrum of the Cs 3d core bands for the covered and plasma exposed sample parts measured at the surface (0 nm) and after a fluence of  $3.59 \times 10^{16} \text{Ar}^+$  ions (evaluated depth of 35.3 nm) for the exposed sample part which corresponds to the deepest measurement performed during this study. The location of the 3d 5/2 bands is indicated for Cs, Cs<sub>2</sub>O and CsOH. The spectra are separated by a constant count offset for readability.

and due to air contamination which occurred before the sample installation into the chamber, the measured WF was larger than 5 eV. The sample was then exposed for 5 mins to an hydrogen discharge operated at 10 Pa pressure, 250 W of injected RF power, which corresponds to a positive ion flux of  $1 \times 10^{20} \text{m}^{-2} \cdot \text{s}^{-1}$  representing 10% of what is measured in negative ion sources for fusion. The sample was floating with a difference between the plasma and floating potential of 8 V. A decrease of the WF to 3.9 eV was then observed, likely due to a reduction of the oxides and cleaning of adsorbed impurities generated by air contamination. This value is in good agreement with the rough estimate determined previously [11] and for which the sample showed a similar surface Cs atomic fraction of 5%. Subsequent plasma exposures led to an increase of the WF to a value of 4.4 eV which corresponds to the pure Mo WF, as can be seen in Figure 1. XPS depth profiles (not shown here) from the exposed sample, showed a strong broadening of the bulk implanted Cs profile and an overall decrease of the Cs amount after plasma exposure. This can be expected, because, as shown in Figure 1, the temperature of the sample increased to more than 200°C and the overall temperature was more than 100°C during at least 2 hours. However and contrary to the bulk, the surface Cs atomic concentration remained constant at a value of around 5%, which cannot then explain the observed decrease of the WF.

To understand why the WF decreased after plasma

exposure, although no drastic change of the Cs surface atomic concentration had been observed, high-resolution XPS of the Mo, O and Cs valence bands were compared between the part of the sample exposed to the plasma and the part shielded by the stainless steel cover. The XPS apparatus was calibrated on Au and Ag samples, and the sputtering was made by  $\text{Ar}^+$  ions accelerated at 10 kV with 20° off normal incidence.

Figure 2 presents Mo 3d valence bands [14] obtained on the surface for the plasma exposed and covered part, as well as the profile measured after a fluence of  $3.59 \times 10^{16} \text{Ar}^+$  ions (evaluated depth of 35.3 nm) for the exposed part only, as the spectrum recorded at the same depth on the covered sample is strictly identical in terms of bands positions and intensity. The pure Mo valence bands are recovered, as expected, at a certain depth. In our study the first fluence step after which this occurred was 35.3 nm (fluence  $3.59 \times 10^{16} \text{Ar}^+$  ions). For both surfaces, one observes  $\text{Mo}_2\text{O}_5$  and / or  $\text{H}_2\text{O}$ ,  $\text{MoO}_3$  (+VI) and  $\text{MoO}_2$  (+IV) whose oxidation state is indicated in parenthesis. The  $\text{MoO}_2$  (+IV) valence bands are clearly more pronounced on the exposed sample part than on the covered sample part in Figure 2. To better understand these observations, XPS-sputtering measurements were performed after a fluence of  $1.04 \times 10^{15} \text{Ar}^+$  ions (evaluated depth of 1 nm),  $3.12 \times 10^{15} \text{Ar}^+$  ions (evaluated depth of 3 nm) and  $1.30 \times 10^{16} \text{Ar}^+$  ions (evaluated depth of 13 nm) for the Figures 3 a), b) and c) and the Mo 3d valence bands and in Figures 3 d), e) and f) for the O 1s valence bands for both the plasma exposed and covered sample parts. Figure 3 a) shows that at an evaluated depth of 1 nm, the exposed sample shows more  $\text{MoO}_2$  (+IV) oxides than the covered sample part, confirming the result from Figure 2. It is associated at the same evaluated depth of 1 nm in Figure 3 d) by a stronger  $\text{H}_2\text{O}$  valence band contribution. For greater depths, one observes a shift of the Mo 3d spectrum towards the pure Mo in Figures 3 b) and 3 d), due to the disappearance of Mo oxides, correlated with a decrease of the  $\text{H}_2\text{O}$  valence band in Figure 3 f). Very likely, the formation of  $\text{MoO}_2$  (+IV) occurs around room temperature following the channel [15]:



That means that  $x$  hydrogen atoms intercalate into  $\text{MoO}_3$  forming  $\text{H}_x\text{MoO}_3$  which in turn slowly decomposes into  $\text{MoO}_2$  and  $\text{H}_2\text{O}$ . As a consequence, the fact that the plasma exposed sample part always shows a more prominent  $\text{MoO}_2$  (+IV) valence band, as observed in Figures 2, 3 a), and 3 b) that is always correlated with a larger quantity of  $\text{H}_2\text{O}$  is a strong hint that the hydrogen plasma positive ions  $\text{H}_x^+$  and neutrals  $\text{H}^0$  reduce the  $\text{MoO}_3$  oxides to  $\text{MoO}_2$  by the channel shown in eq. (1). More importantly, one can see that for the parameters chosen for this study, the plasma positive ions (neutralized near the surface by 2 photon Auger process) and neutrals

diffusing into the Mo bulk, the reaction shown in eq. (1) occurs up to an evaluated depth of 13 nm, and thus the influence of the plasma is not limited to surface processes only. For greater depths than 13 nm, no difference could be observed between XPS spectra performed on the plasma exposed and covered sample parts.

These results could also partially be explained by an air contamination, but since similar spectra to the ones in Figure 3 have been systematically observed for all the XPS spectrum until a depth of 13 nm, this hypothesis is likely to be ruled out. Nevertheless, it is possible to discriminate by thermodesorption the amount of  $\text{H}_2\text{O}$  due to air contamination from the water generated by  $\text{MoO}_3$  reduction by performing the same experiment with a deuterium plasma: in this case, the  $\text{D}_2\text{O}$  will originate from the reduction induced by the plasma only, while  $\text{H}_2\text{O}$  will be due to air contamination.

The Figure 4 shows a high-resolution XPS spectrum of the 3d Cs valence bands. As it can be seen on this panel, only oxidized Cs and Cs hydrides are present, due to air contamination.

We conclude from this study that:

- hydrogen plasma reduces the  $\text{MoO}_3$  oxides to  $\text{MoO}_2$  oxides with generation of  $\text{H}_2\text{O}$ ,
- hydrogen plasma species influence the material to an evaluated depth of roughly 13 nm under the present conditions,
- under the present experimental conditions, the presence of  $\text{H}_2\text{O}$ , together with the diffusion of the Cs due to the sample high temperature measured during plasma pulses are the possible causes of the WF increase.

Finally, it may be possible to mitigate the diffusion of Cs and thus the WF increase by keeping the sample at a low temperature that should be determined by experiments.

**Acknowledgments.** – This work has been carried out within the framework of the EUROfusion Consortium and has received funding from the Euratom research and training programme 2014-2018 and 2019-2020 under grant agreement No 633053. The views and opinions expressed herein do not necessarily reflect those of the European Commission.

**Data Availability.** – The data that support the findings of this study are available from EUROfusion. Restrictions apply to the availability of these data, which were used under license for this study. Data are available from the authors upon reasonable request and with the permission of EUROfusion.

## REFERENCES

- [1] Speth E. et al., Nucl. Fus. 46 (2006) 220.
- [2] B. Heinemann, H.-D. Falter, U. Fantz, P. Franzen, M. Froeschle, W. Kraus, C. Martens, R. Nocentini, R. Riedl, E. Speth et A. Staebler, Fusion Eng. and Design, 86, 6 (2011) 768.
- [3] V. Toigo et al., Nucl. Fusion, 57, 8 (2017) 086027.
- [4] V Toigo et al., New Journal of Physics, 19, 8, (2017) 085004.
- [5] Belchenko Yu. I., Dimov G. I., and Dudnikov V. G., Nucl. Fus. 14 (1974) 113-114.
- [6] V. G. Dudnikov, Rev. Sci. Inst., vol. 63, no. 4 (1992) 2660.
- [7] Schiesko L. et al., Plas. Phys. & Cont. Fus. 53 (2011) 085029.
- [8] Franzen P. and Fantz U., Fus. Eng. & Design 89, (2014) 2594.
- [9] Cristofaro S., Fröschle M., Mimo A., Rizzolo A., De Muri M., Barbisan M. and Fantz U., Rev. Sci. Inst. 90 (2019) 113504.
- [10] L. Schiesko, G. Cartry, C. Hopf, T. Höschen, G. Meisl, O. Encke, P. Franzen, B. Heinemann, K. Achkasov, C. Hopf et U. Fantz, AIP Conf. Proc., 1655, 1, (2015) 020003.
- [11] L. Schiesko, G. Cartry, C. Hopf, T. Höschen, G. Meisl, O. Encke, B. Heinemann, K. Achkasov, P. Amsalem et U. Fantz, J. App. Phys., 118, 7, (2015) 073303.
- [12] R. Friedl and U. Fantz, J. App. Phys., 122, (2017) 083304.
- [13] R. H. Fowler, Phys. Rev., 38 (1931) 45.
- [14] J. Baltrusaitis, B. Mendoza-Sanchez et al., Appl. Surf. Sci., 326 (2015) 151.
- [15] A. Borgschulte, O. Sambalova et al., Sci. Rep., 7 (2017) 40761.